RSC Advances

ROYAL SOCIETY OF CHEMISTRY

www.rsc.org/advances

Etching of unmodified Au@Ag nanorods: a tunable colorimetric visualization for rapid and high selective detection of Hg^{2+}

Rong Yang[†], Dan Song[†], Chongwen Wang[‡], Anna Zhu[†], Rui Xiao[‡], Jingquan Liu[†], Feng Long[†*]

[†]School of Environment and Natural Resources, Renmin University of China, 100872, Beijing,

[‡]Beijing Institute of Radiation Medicine, Beijing 100850, China

[*]Corresponding Author: longf04@ruc.edu.cn

Abstract: A simple and cost-effective colorimetric approach based on unmodified Au@Ag nanorods (Au@Ag NRs) was developed for Hg^{2+} detection. Unmodified Au@Ag NRs with different Ag nanoshell thicknesses served as the signal readout because the Ag coating-induced blueshift and enhancement of the longitudinal plasmon of Au NRs resulted in abundant and tunable optical absorptions in the visible region. The etching sensing mechanism was revealed to be related to the redox reaction between Hg^{2+} and the Ag nanoshell of Au@Ag NRs. The Ag nanoshell of Au@Ag NRs gradually etched from the ends as the Hg^{2+} concentration was gradually increased and shoulder shapes formed, and then disappeared. The Hg^{2+} concentration-dependent color of Au@Ag NRs with a thick Ag nanoshell thickness changed from brownish-red to light-red, light-violet, and to colorless. The limit of detection (LOD) and detection range of Hg^{2+} became tunable as the Ag nanoshell thickness was increased, and the lowest LOD was 10 nM. A dip located between two strong absorption peaks was observed when Au@Ag NRs with a thick Ag nanoshell thickness was used. The change in this dip provided a new sensor parameter for Hg^{2+} detection on the basis of absorption spectra. The proposed method also showed high selectivity toward Hg^{2+} over other metal ions. The Au@Ag NR detection system can detect even a low Hg^{2+} concentrations in drinking water.

Introduction

Substantial sensing techniques based on noble metal nanoparticles (NPs) have attracted considerable attention because of their unique optical properties. Au NP-based optical sensing method, such as colorimetry, light-scattering, and fluorescence, have been widely designed and applied for contaminants detection.[1,2] Colorimetric detection induced by localized surface plasmon resonance (LSPR) is commonly used because of its simplificity, convenience, and visibility requiring the naked eye only.[2-4] The color change of metal NP solutions associated with LSPR relies on NP size, shape, interparticle distance, and local dielectric environment.[1-3,5] Given their transverse and longitudinal LSPR adsorption modes induced by the oscillation of conduction electrons along two directions, Au nanorods (Au NRs) enrich the color change of Au nanoprobes.[5-7] Recent studies have extensively applied Au NRs in the colorimetric sensing of metal ions, DNA, proteins, and small molecules based on the aggregation of Au NRs.[1-8] Compared with Au NPs, Ag NPs produce a much stronger and sharper plasmon resonance.[9,10] Meanwhile, the LSPR absorption band of Ag NPs with a well-controlled size changes more easily than Au NPs when exposed to special targets. The strong shape-dependent optical properties of Ag NPs allow the rapid, sensitive, and visualized detection of targets with minimal consumption of materials.[4,11,12] Various shaped Ag NPs, such as nanoprisms, spherical, and nanoclusters, have been considered for the colorimetric detection of different target molecules on the basis of morphology transition.[9-12] An Ag nanoprisms-based sensor has been applied to detect Hg^{2+} on the basis of its morphological transition from nanoprism to sphere after Hg^{2+} etching.[12] However, the precise controlling of Ag NPs morphology remains a challenge.

Hg^{2+}, a highly biologically toxic and ubiquitous heavy metal ion, is a stable inorganic form of Hg in the environment and organisms.[13] The traditional technologies for Hg^{2+} analysis include instrumental and sensor methods. Instrumental analysis methods such as atomic absorption spectroscopy, inductively coupled plasma mass spectrometry, and selective cold vapor atomic fluorescence spectrometry are more precise than other methods, but they required expensive equipment, high operational cost, and laborious procedures.[14-15] Numerous remarkable sensors based on organic molecules, polymeric materials, biomaterials, and semiconductor nanocrystals have been recently developed for Hg^{2+} detection using optical and electrochemical signals.[11,12,16-21] However, these sensors generally require complex material preparation or

biomolecule conjugation processes.

Colorimetric sensors designed by generating a nanoshell on the surface of the inner core exhibit more brilliant color changes than colorimetric detection systems based on the aggregation of Au NRs and the morphology transition of Ag NPs.[7,22] The Ag coating-induced blueshift and enhancement of the longitudinal LSPR of Au NRs result in abundant and tunable optical absorptions in the visible region, making the Au@Ag core-shell NRs (Au@Ag NRs) a feasible candidate for colorimetric sensing.[7,8,19] Au@Ag NRs are easy to prepare and their LSPR properties can be easily controlled by changing the size and shape of the core and the thickness of the shell. Considering the previously reported interaction mechanism between Hg^{2+} and Ag NPs,[11,12] we assumed that Au@Ag NRs are highly suitable for Hg^{2+} detection because of their controllable monodispersity and aspect ratio, broad plasmon resonance tenability from the near-UV to IR region, and increased sharpness and strength of longitudinal SPR bands.[7,8,19,20] Although a general method has been developed to tune the dynamic range of biosensors for the detection of heavy metal ions, no such method has been reported for colorimetric nanosensors. The current study developed a simple, rapid, sensitive and selective colorimetric assay of Hg^{2+} based on unmodified Au@Ag NRs; Ag nanoshell with different thickness were introduced into Au NRs to confer the assay a tunable dynamic range. The etching mechanism of Au@Ag NRs by Hg^{2+} was analyzed through UV-vis spectroscopy, high-resolution transmission electron microscopy (HR-TEM), and energy dispersive X-ray spectroscopy (EDS). The developed method was also successfully used to detect Hg^{2+} in drinking water samples.

Experimental section

Reagents and apparatus. Gold chloride trihydrate ($HAuCl_4$), Cetyltrimethyl ammonium bromide (CTAB), Sodium borohydride ($NaBH_4$), silver nitrate ($AgNO_3$), and ascorbic acid (AA) were purchased from Sigma-Aldrich. Hydrochloric acid (HCl), sodium hydroxide (NaOH), $Pb(NO_3)_2$, $MnCl_2$, $AlCl_3$, $CuCl_2$, $FeSO_4$, $Hg(NO)_3$, $CdCl_2$, $CoCl_2$, $CaCl_2$, and $Mg(NO_3)_2$ were purchased from Beijing Chemical Works (China). All the reagents were of analytical grade and were used without further purification. The ultrapure water with a resistivity of 18.2 MΩ, obtained from a Millipore water purification system (Milli-Q, Millipore, USA), was used in all experiments.

All the absorption spectra were performed on a Shimadzu UV-3150 spectrometer (Japan) or a NanoDrop 2000 (Thermo, USA). HR-TEM images with an accelerating voltage of 200 kV and

EDS spectra were obtained using a JEM-2100F transmission electron microscope. Samples dispersed at an appropriate concentration were cast onto a carbon-coated copper grid. A PB-10 pH meter (Sartorious, Germany) was employed to measure pH values of all the aqueous solutions.

Preparation of Au@Ag NRs with different Ag nanoshell thicknesses. Au NRs were synthesized using the silver ion-assisted, seed mediated method as previously described.[23] In brief, the seed solution was initially prepared by mixing 5 mL of 0.1 M CTAB solution with 42 μL of 29 mM $HAuCl_4$, and 0.3 mL of 10 mM $NaBH_4$ with vigorous stirring for 10 min. Then, the mixture of 0.4 mL of 10 mM $AgNO_3$ and 40 mL of 0.1 M CTAB solution was added with 0.8 mL of 29 mM $HAuCl_4$. After 0.32 mL of 0.1 M ascorbic acid was added with gentle mixing, 130 μL of the seed solution was added. The mixture was kept at 30 ºC overnight without any further stirring. The as-prepared Au NRs (Figure S1) were further purified twice via centrifugation at 9000 rpm for 10 min to remove any excess reagents, and then used to prepare of Ag@Au NRs. The synthesized Au NRs had a UV-vis absorbance at 830 nm (Figure S1).

Au@Ag NRs were prepared as previously described with some modifications.[24] In brief, 2 mL of Au NR solution was added to 4 mL of 0.04 M CTAB aqueous solution with vigorous stirring at 28 ºC. Up to 130 μL of 0.1 M ascorbic acid, varying amounts of 1 mM $AgNO_3$, and 240 μL of 0.1 M NaOH were sequentially added. Au@Ag NRs with various Ag nanoshell thicknesses were prepared by tuning the amount of $AgNO_3$. The color of the solution gradually changed in 2 min, indicating the formation of Au@Ag NRs. The Au@Ag NR solution was purified and then concentrated to 2 mL with deionized water.

Analysis of Hg^{2+} based on unmodified Au@Ag NRs. Various Hg^{2+} concentrations (0-267 μM) were added to 1 mL of Au@Ag NR solution, and a different volume of ultrapure water was added to ensure that the total volume was the same. The resulting solution was stored at room temperature for 5 min. A quantitative analysis was performed and the absorption spectra of the mixture were recorded under the same conditions. All experiments were performed in triplicate.

To evaluate the potential matrix effects of environmental samples on Hg^{2+} detection, spiked samples of tap water and commercially available bottled water were tested at concentrations of 0.6, 1.0, and 2 μM. The specificity of the sensor was assessed by evaluating its responses to such potentially interfering metal ions, such as Cu^{2+}, Mg^{2+}, Cd^{2+}, Al^{3+}, Co^{2+}, Mn^{2+}, Pb^{2+}, Ca^{2+}, Zn^{2+}, Fe^{2+}, Fe^{3+}, and Ag^{+} at concentrations up to 1 mM.

Results and discussion

Characterization of Au@Ag NRs with different Ag nanoshell thicknesses. Au NRs with a longitudinal SPR peak at 830 nm and a transverse peak at 576 nm were selected as the core, which had uniform size distribution and good dispersity (Figure S1). For colorimetric detection, the target induced spectral shifts that lead to a visually detectable color change were the primary consideration, and the most sensitive region of color perception for the naked eye was at 500 nm to 600 nm.[25,26] Although the longitudinal SPR of the Au NRs was not within this range, Ag coating triggered the blueshift of the longitudinal LSPR of Au NRs. Furthermore, the plasmonic line width of the Au@Ag NRs was narrower than that of the original Au NRs.[27] This phenomenon, known as 'plasmonic focusing', makes Au@Ag NRs more suitable for a high-quality colorimetrical sensor.[27] The thickness of the Ag nanoshell can be easily controlled by tuning the amounts of silver nitrate and ascorbic acid. In this study, Au@Ag NRs with thin moderate, and thick Ag nanoshell thickness were prepared, and denoted as Au@Ag-NR1 (~2.1 nm), Au@Ag-NR2 (~5.8 nm), and Au@Ag-NR3 (~9.5 nm), respectively (Figure 1a). As shown in the insets of Figure 1b, the color of Au@Ag NR colloid gradually changed from dark-yellow to green to brownish-red and the plasmon resonance of the Au@Ag NRs relocated from 687 nm to 572 nm as the Ag nanoshell thickness was increased. Four SPR peaks could be observed and were designated as peaks 1 to 4 from long to short wavelength. Peak 1 and peak 3 with a remarkable intensity and fine tenability corresponded to the longitudinal and transverse SPR peak of NRs, respectively. As Ag nanoshell thickness on the Au NRs was increased, peak 1 exhibited a remarkable blueshift accompanied with an enhanced absorbance intensity, whereas peak 3 exhibited a remarkable redshift accompanied with an enhanced absorbance intensity. Peaks 2 and 3 Au@Ag-NR3 merged, and a deep dip between peaks 1 and 3 appeared. Figure 1b-d illustrate the change in thickness of the Ag nanoshell in the Au@Ag NRs.

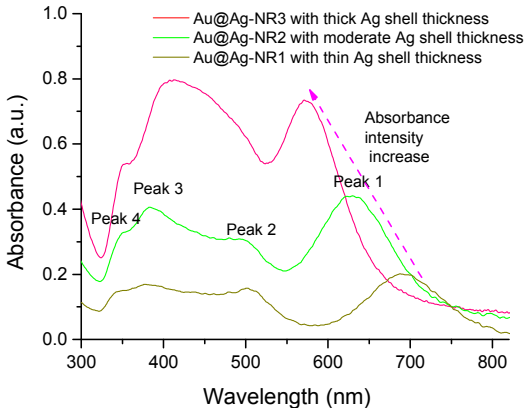

(a)

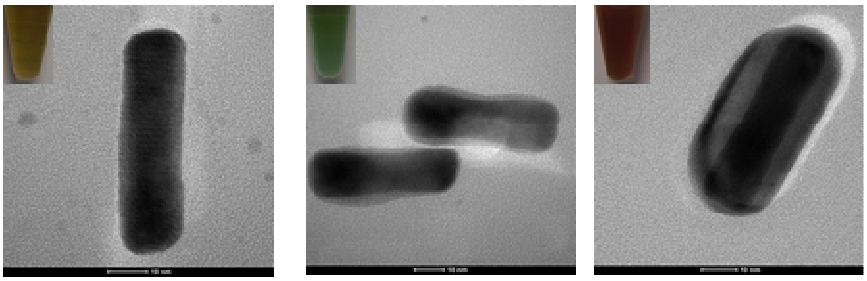

(b) (c) (d)

Figure 1. (a) Absorption spectra of Au@Ag NRs with different Ag nanoshell thicknesses. Typical TEM images of Au@Ag NRs with a (b) thin, (c) moderate, and (d) thick Ag nanoshells, respectively. Insets: the corresponding colors of the Au@Ag NRs colloid with different Ag nanoshell thicknesses.

Sensing mechanism of Hg^{2+} detection based on Au@Ag NR etching. Synthesized Au@Ag NRs present excellent optical properties because of the distinct surface plasmon resonance (SPR) absorption band in the visible region, which is beneficial for the colorimetrical detection of targets. The proposed etching mechanism of Au@Ag NRs by Hg^{2+} is demonstrated in Figure 2a. The etching process was initially inspected using UV-vis spectrometry. Au@Ag-NR3 was used as a model to investigate the interaction between Hg^{2+} and Au@Ag NRs. The solution color was altered from brownish-red to light-red after adding the Hg^{2+} solution to the as-prepared Au@Ag-NR3 solution. The color continued to change from light-red to light-violet in response to a further increase of the Hg^{2+} concentration (inset of Figures 2b-2d). The color of the Au@Ag-NR2 colloid was also gradually changed as the Hg^{2+} concentration was increased (Figure S2). As shown in Figure 3b, the absorbance intensity decreased and the LSPR peak slightly blueshifted in presence of low Hg^{2+} concentrations in the solution. The Au@Ag-NR3 solution turned to light-violet when the Hg^{2+} concentration exceeded 87 μM. This results indicated that the absorbance intensity obviously decrease and the LSPR peak slightly redshifted. The spectra shift and intensity decrease of peak 1 can be attributed to the presence of Hg^{2+} and reveal the SPR change of the Au@Ag NRs, which greatly contribute to the color change. Hg^{2+} and Au@Ag NRs could interact in a short time (<2 min) on the surface of Au@Ag NRs. After incubating the mixture of Hg^{2+} and Au@Ag NRs for 2 min, the color of the mixture did not change again even if it was stored at room temperature for a week (data not shown). The mixture stability is essential for the accurate and visualized detection of Hg^{2+}. The following redox reaction occurs between zero-valent Ag and Hg^{2+} with standard potentials of 0.8 V (Ag^{+}/Ag) and 0.85 V (Hg^{2+}/Hg).

$$Ag_n + Hg^{2+} \leftrightarrow Ag_{n-2}Hg + 2Ag^{+} \quad (1)$$

This redox reaction led to the etching of nano-Ag and the formation of Ag-Hg nanoalloy on the surface of Au@Ag NRs. The etching mechanism was analyzed via TEM and EDS in addition to UV-vis spectroscopy (Figure 2c-2e). TEM images demonstrate that the color changes of Au@Ag NRs can be attributed to their morphological transition as the etching process continued. This observation was demonstrated by revealing shoulder shapes (Figure 2d, with 5 μM Hg^{2+}), and etching-cylindrical shapes (Figure 2e, with 65 μM Hg^{2+}) in the presence of Hg^{2+} and the original cylindrical shapes (Figure 2c) in the absence of Hg^{2+}. Interestingly, the Ag nanoshell of the Au@Ag NRs was gradually etched from the end of the NRs (Figure 2c-2e) as Hg^{2+} concentration increased. The morphology transition of the Au@Ag NRs can be ascribed to the

following reasons. First, the active Ag atoms at both ends of the Au@Ag NRs easily to be coordinated with Hg^{2+} and separated from the original nanostructure. On basis of the Gibbs-Thomson effect, a convex surface has a higher surface energy than a flat surface.[27] Both ends of the Au@Ag NRs have a higher surface energy than their lateral sides. On the other hand, the Ag atoms at the end areas have a higher coordination number than the lateral sides, which results in higher surface energy in these areas.[12] Therefore, the ends of Au@Ag NRs are more prone to etching rather than other areas. On the other hand, the as-prepared Au@Ag NRs were surrounded by a small amount of positively charged CTAB molecules. More CTAB molecules were on the lateral side than on the end; as a result, more Hg^{2+} ions were adsorbed on the latter than the former because of electrostatic repulsion, thus accelerating the etching of the ends of the Au@Ag NRs, which caused the distinct changes in the absorption spectra.

Freshly generated Hg atoms can strongly bond on the Ag surface, which accounts for the slight blueshift of the SPR band of Ag NPs. The shape change of the Au@Ag NRs in the presence of Hg^{2+} indicates the reduction of Hg(II) to Hg(0) and thus the formation of the amalgam of Hg and Ag wrapping around the Au@Ag NRs.[29] To further verify the interaction between Au@Ag NRs and Hg^{2+}, the EDS in STEM was used to characterize the elemental identity of Au@Ag NRs after adding low concentration (1 μM) and high concentration (30 μM) of Hg^{2+}. The EDS has been recently proven to be a powerful technique in analyzing the elemental identity and location of atomic columns in nanomaterials at atomic resolution.[30] The results of the EDS elemental analyses are summarised in Table 1 and shown in Figure S3. Hg^{2+} appeared on the surface of the Au@Ag NRs after Hg^{2+} reacted with Au@Ag NRs. The amount of Hg^{2+} increased and the amount of Ag decreased on the surface of Au@Ag NRs. This finding is consistent with the TEM images and UV-vis spectra of Au@Ag NRs. These observations are also agree with those of previous results that demonstrated the formation of an Hg nanoshell on the surface of an Ag nanoshell after Hg^{2+} action, which is attributed to the formation of the amalgam of Ag and Hg.[12] However, the etching mechanism of the Au@Ag NRs by Hg^{2+} is never reported. In accordance with the proposed etching mechanism of Hg^{2+}, the change in the absorption spectra caused the color change of the Au@Ag NR colloids in presence of Hg^{2+}. Furthermore, we proved that the effect of pH on the absorption spectra of the Au@Ag NRs was insignificant when the pH was higher than 2 (Figure S4). Thus, the colorimetric detection of Hg^{2+} can be realized.

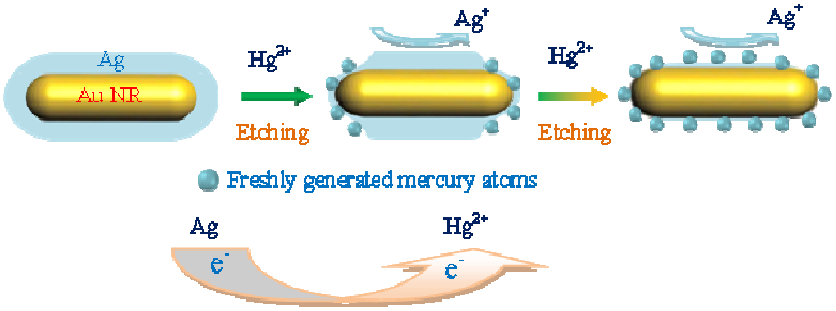

(a)

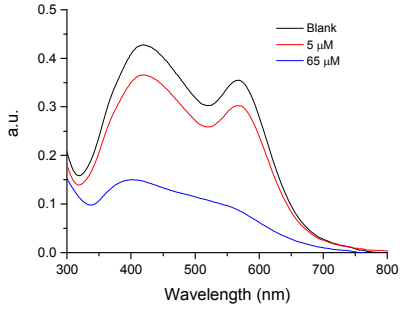

(b)

(c) (d) (e)

Figure 2. Etching mechanism of Au@Ag NRs by Hg^{2+}. (a) Scheme of Au@Ag NR Etching mechanism. (b) Absorption spectra of Au@Ag NRs without Hg^{2+} and with different concentrations of Hg^{2+} (5 μM or 65μM). TEM images of (c) original Au@Ag NRs, (d) Au@Ag NRs etched by a low concentration of Hg^{2+} (5 μM), and (e) Au@Ag NRs etched by a high concentration of Hg^{2+} (65 μM), respectively. Inset: the corresponding colors of the Au@Ag NR solution with different Hg^{2+} concentration.

Table 1 EDS spectral analysis of Au@Ag NRs upon the addition of Hg^{2+} of low concentration (5 μM) or high concentration (30 μM).

Hg^{2+} concentration	Element	Weight (%)	Atomic (%)	Uncert. (%)	Correction	k-Factor
Low	Ag(K)	21.47	33.32	1.43	0.98	6.491
	Au(L)	73.69	62.64	1.93	0.75	5.653
	Hg(L)	4.83	4.03	0.70	0.75	5.824
High	Ag(K)	13.23	21.82	0.86	0.98	6.491
	Au(L)	76.24	68.85	1.55	0.75	5.653
	Hg(L)	10.51	9.32	0.65	0.75	5.824

Dose-responses of Hg^{2+} using Au@Ag NRs with different Ag nanoshell thicknesses. The absorption spectra of Au@Ag-NR1, Au@Ag-NR2, and Au@Ag-NR3 upon the addition of different Hg^{2+} concentrations were compared to investigate the effect of the Ag nanoshell thickness of Au@Ag NRs on Hg^{2+} detection. Figures 3a-3c display the absorption spectra of the interaction between Au@Ag NRs and Hg^{2+} at concentrations ranging from 0 to 267 μM. For Au@Ag-NR1 and Au@Ag-NR2, the absorbance intensity gradually reduced as the Hg^{2+} concentration was gradually increased, and the wavelength of peak 1 blueshifted when the Hg^{2+} concentration was not too high. However, the wavelength of peak 1 redshifted when the Hg^{2+} concentration exceeded 33 μM. This phenomenon should contribute to the LSPR of Au NRs caused by the complete etching of the Ag nanoshell of the Au@Ag NRs. After the addition of Hg^{2+} solution to the prepared Au@Ag-NR1 solution, the color of Au@Ag-NR1 solution change from orange-yellow to light-violet, and its absorbance intensity decreased as the Hg^{2+} concentration was increased (inset of Figure 3a). The Hg^{2+} detection system based on Au@Ag-NR1 showed a linear response at 0.6 μM to 20 μM and a detection limit of 10 nM based on 3 σ/slope (where σ is the standard deviation of the blank samples) (Figure 3d). This detection limit is comparable to that of some reported colorimetrical sensors for Hg^{2+},[3,11,12,31] and satisfies the requirement of drinking water standards in the USA.[32] The introduction of Hg^{2+} to Au@Ag-NR2 decreased the absorbance intensity, and changed the color (inset of Figure 3b). The linear response ranged from 2.0 μM to 30 μM, and the detection limit was 200 nM (Figure 3d).

The absorbance intensity of peak 3 was slightly higher than that of peak 1 in Au@Ag-NR3 as compared with Au@Ag-NR1 and Au@Ag-NR2. Figure 3c displays the absorption spectra of the interaction between Au@Ag-NR3 and Hg^{2+} at 0 μM to 267 μM. The addition of Hg^{2+} significantly affected the absorbance intensity and peak position of Au@Ag-NR3. The linear response ranged from 5.0 μM to 200 μM and the detection limit was 500 nM (Figure 3d). The results indicate that the sensitivity of the Au@Ag NR-based chemosensor decreases with the increasing Ag nanoshell thickness. Interestingly, the color drastically transitioned from brownish-red to light-red, light-violet, and to colorless (inset of Figure 3c). This color range in Au@Ag-NR3 allows the visualization of color change. Therefore, from the point of view of macroscopic colorimetry, Au@Ag-NR3 is more suitable for direct read-out visualization than

Au@Ag-NR1 and Au@Ag-NR2. Except for the decrease of an absorbance intensity of 580 nm with increasing Hg^{2+} concentration, the absorbance intensity of 412 nm was Hg^{2+} concentration-dependent (Figure S5). However, what attracts us most is the change of the dip located between peak 1 and peak 3. As the Hg^{2+} concentration was increased, the dip wavelength slightly blueshifted and the absorbance intensity is gradually decreased. When the Hg^{2+} concentration was 267 μM, peaks 1 and 3 were merged, and the dip between the two original peaks disappeared and ultimately transformed into a wide peak. The peak wavelength and absorbance intensity of LSPR are commonly used parameters to detect heavy metal ions on the basis of NP absorption spectral analyses. However, the LSPR absorption spectral changes induced by noble metal nanostructures with different morphologies are influenced by other parameters. Abundant spectral signals, such as the dip between the two peaks, the integration of adjacent peaks, and the relative intensity change of different peaks, can be applied to quantify the concentration of targets. These enhance the overall performance of the sensors. Therefore, further exploring the normal spectral lines is essential to obtain new sensor parameters. As demonstrated in Figure 3d, the absorbance intensity of the dip was Hg^{2+} concentration-dependent. Dip is a new sensor parameter located between two strong absorption peak positions that can be used to quantify the target. The Hg^{2+} concentration detection can be detected by using the change of the position and intensity of the dip.

Several studies have reported on the application of Au@Ag NPs as sensors to detect small molecules and metal ions.[3,22,33] However, our proposed approach is different from the previously reported Au@Ag core-shell nanomaterial-based sensors and their sensing properties. The proposed approach is convenient and efficient, and does not need complicated instruments. Only one absorption spectrometer after only 2 min incubation is needed for the proposed approach. Moreover, the proposed sensor can achieve a tunable dynamic range by adjusting the Ag nanoshell thickness of Au@Ag NRs. A practical sensor needs to have a tunable dynamic range that matches the concentration ranges for different locations, because most analytes of interest have varied concentration ranges at different locations in the environment.[34]

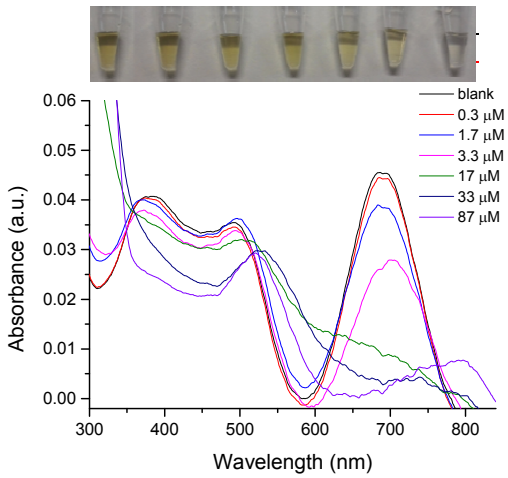

(a)

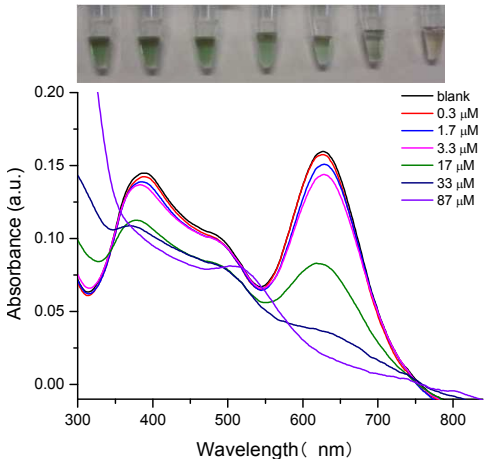

(b)

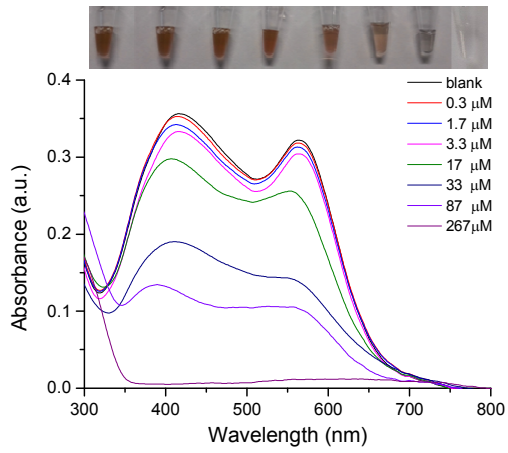

(c)

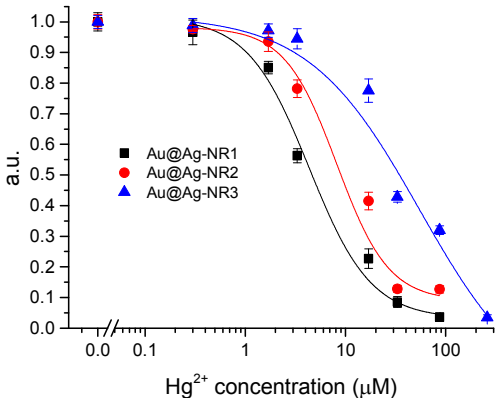

(d)

Figure 3. Effect of the Ag nanoshell thickness of Au@Ag NRs on Hg^{2+} detection. Typical absorbance spectra of Au@Ag NRs with a (a) thin, (b) moderate, and (c) thick Ag nanoshell thickness mixed with different Hg^{2+} concentrations, respectively. Insets: the corresponding colors of the Au@Ag NR solution with different Hg^{2+} concentrations. (d) Dose-response curves of Hg^{2+} detection with Au@Ag-NR1, Au@Ag-NR2, and Au@Ag-NR3. The presented values are the average of three independent experimental results.

Selectivity of Ag@Au NR-based sensor. To assess the selectivity of the unmodified Ag@Au NR-based sensor, other metal ions (Cu^{2+}, Mg^{2+}, Cd^{2+}, Al^{3+}, Co^{2+}, Mn^{2+}, Pb^{2+}, Ca^{2+}, Zn^{2+}, Fe^{2+}, Fe^{3+}, and Ag^{+}) at concentrations up to 1 mM were added into Ag@Au-NR3 solution under the same conditions. Figure 4 showed the interaction of between freshly prepared Ag@Au NRs and various metal ions, and their color change. The solution contacting Hg^{2+} changes from brownish-red to colorless, while other alkaline earth metals (Mg^{2+}, Ca^{2+}) and transition-metal ions (Ni^{2+}, Mn^{2+}, Cu^{2+}, Zn^{2+}, Co^{2+}, Cd^{2+}, Fe^{2+}, Fe^{3+}, and Ag^{+}) exerted negligible effects on the color and SPR band of the Ag@Au NR solution. This result indicates that the Ag@Au NR-based assay approach is highly selective toward Hg^{2+} but not to other transition-metal and alkaline metal ions under similar conditions. The specific Hg^{2+} detection can be mainly attributed to the specific etching ability of Hg^{2+} to Ag@Au NRs. Different Hg types, including Hg, Hg $(OH)_2$, HgO, CH_3Hg^{+} and CH_3HgCl, can be transformed into Hg^{2+} ions by using a digestive method.[31] Thus the proposed probe may offer a great promise as a colorimetric detection method for total Hg forms.

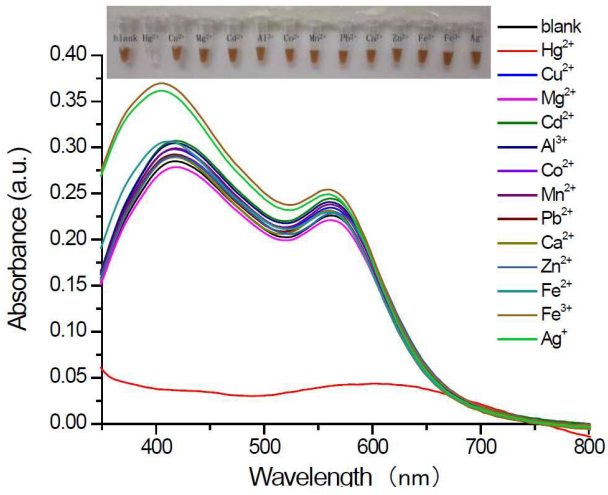

Figure 4. Selectivity of Ag@Au NR-based sensing system. The concentration of Mg^{2+}, Ca^{2+}, Ni^{2+}, Mn^{2+}, Cu^{2+}, Zn^{2+}, Co^{2+}, Cd^{2+}, Fe^{2+}, Fe^{3+}, or Ag^{+} is 1 mM, and the concentration of Hg^{2+} is 200 μM. Insets: the corresponding colors of the Au@Ag NR solution upon the addition of different heavy metal ions.

Determination of Hg^{2+} in drinking water samples. The applications of the proposed colorimetric sensor based on unmodified Au@Ag NRs were evaluated to determine Hg^{2+} in real samples, such as tap water and commercially available bottled water. The water samples were spiked with different Hg^{2+} concentrations. The results summarized in Table 2 agree with the expected values. The recovery of all measured samples was between 90% and 115%, and the parallel tests showed that the relativity coefficient (the relative ratio of the standard deviation σ to the mean μ) was within 1.78% to 5.4% (n=2).[35] These results indicate that any possible interference from the different background compositions of water samples on the Au@Ag NR-based sensing system was negligible. Therefore, the developed method can be successfully applied to Hg^{2+} analysis in drinking water samples.

542 **Table 2** Determination of Hg^{2+} in drinking water samples using the proposed method

Samples	Spiked concentration (μM)	Detection concentration (μM)	Recovery (%)	CV (%)
Bottled water	0.6	0.58	96.7	3.56
	1.0	0.92	92.0	3.78
	2.0	2.11	105.5	1.78
Tap water	0.6	0.67	111	3.56
	1.0	0.97	97.0	5.4
	2.0	2.16	108	3.23

543

544

545

546

547

548

549

550

551

552

553

554

555

556

557

558

In summary, we developed a simple and cost-effective colorimetrical approach for the rapid and highly selective detection of Hg^{2+} based from the etching mechanism of unmodified Au@Ag NRs by Hg^{2+}. This simple and rapid method showed detection limits as low as 10 nM for Hg^{2+}, as well as high selectivity toward Hg^{2+} over other metal ions. Our proposed approach has several advantages over other colorimetrical sensors for Hg^{2+} detection. First, the present method only requires unmodified Au@Ag NRs as the detection material. Second, the whole detection process is time-saving (<2 min), and the color changes of the Au@Ag NR solution upon the addition of Hg^{2+} are visible with the naked eye. Third, the detection system only requires one absorption spectrometer. The proposed sensor can also achieve a tunable dynamic range by adjusting the Ag nanoshell thickness of Au@Ag NRs. We believe that this method could provide new breakthroughs in Hg^{2+} detection in drinking water.

■ AUTHOR INFORMATION

Corresponding Author

*E-mail: longf04@ruc.edu.cn.

■ ACKNOWLEDGMENT

This research was financially supported by the National Natural Science Foundation of China (21077063, 21277173), the National Instrument Major Project of China (2012YQ3011105), the Special Fund of State Key Joint Laboratory of Environment Simulation and Pollution Control (14K01ESPCT), and the Basic Research Funds in Renmin University of China from the Central Government (13XNLJ01).

References:

(1) Ray, P. C. *Chem. Rev.* **2010**, *110*, 5332.

(2) Saha, K.; Agasti, S. S.; Kim, C.; Li, X.; Rotello, V. M. *Chem. Rev.* **2012**, *112*, 2739.

(3) Du, J.; Jiang, L.; Shao, Q.; Liu, X.; Marks, R.S.; Ma, J.; Chen, X. *Small* **2013**, *9*, 1467-1481.

(4) Tan, K.; Yang, G.; Chen, H.; Shen, P.; Huang, Y.; Xia, Y. *Biosens. Bioelectron.* **2014**, *59*, 227-232.

(5) Jayabal, S.; Pandikumar, A.; Lim, H. N.; Ramaraj, R.; Sund, T.; Huang, N. M. *Analyst* **2015**, *140*, 2540-2555.

(6) Huang, X.; Neretina, S.; El-Sayed, M. A. *Adv. Mater.* **2009**, *21*, 4880-4910.

(7) Sau, T. K.; Rogach, A. L.; Jackel, F.; Klar, T. A.; Feldmann, J. *Adv. Mater.* **2010**, *22*, 1805.

(8) Zhang, F.; Zhu, J.; Li, J. J.; Zhao, J. W. *J. Mater. Chem. C* **2015**, *3*, 603-6045.

(9) Yang, X.; Yu, Y.; Gao, Z. *ACS Nano* **2014**, *8*, 4902-4907.

(10) Xue, B.; Wang, D.; Zuo, J.; Kong, X.; Zhang, Y.; Liu, X.; Tu, L.; Chang, Y.; Li, C.; Wu, F.; Zeng, Q.; Zhao, H.; Zhao, H.; Zhang, H. *Nanoscale* **2015**, *7*, 8048-8057.

(11) Farhadia, K.; Forough, M.; Molaei, R.; Hajizadeh, S.; Rafipour, A. *Sens. Actuators B* **2012**,*161*, 880-885.

(12) Chen, L.; Fu, X.; Lu, W.; Chen, L. *ACS Appl. Mater. Interfaces* **2013**, *5*, 284-290.

(13) Harris, H.H.; Pickering, I.J.; George, G.N. *Science* **2003**, *301*, 1203.

(14) Ashoka, S.; Peake, B. M.; Bremner, G.; Hageman, K. J.; Reid, M. R. *Anal. Chim. Acta* **2009**, *653*, 191-199.

(15) Yuan, C. G.; Wang, J.; Jin, Y. *Microchim Acta* **2012**, *177*, 153-158.

(16) Aragay, G.; Pons, J.; Merkoci, A. *Chem. Rev.* **2011**,*111*, 3433-3458.

(17) Wang, F. H.; Cheng, C. W.; Duan, L. C.; Wu L.; Xia, M. Z.; Wang, F. Y. Sens. Actuators B 2015, 206, 679-683.

(18) Kumar, D. N.; Rajeshwari, A.; Alex, S. A.; Chandrasekaran, N.; Mukherjee, A. *New J. Chem.* **2015**, *39*, 1172-1178.

(19) Lee, J. S.; Han, M. S.; Mirkin, C. A. *Angew. Chem. Int. Ed.* **2007**, *46*, 4093-4096.

(20) Zhang, X.; Zhu,Y. Y. *Sens. Actuators B* **2014**, *202*, 609-614.

(21) Li, L.; Yu, B.; You, T. *Biosens. Bioelectron.* **2015**, *74*, 263-269.

(22) Hao, J. R.; Xiong, B.; Cheng, X. D.; He, Y.; Yeung, E. S. *Anal. Chem.* **2014,** *86*, 4663.

(23) Babak, N.; Mostafa, A. E. *Chem. Mater.* **2003**, *15*, 1957-1962.

(24) Xiang, Y. J. *Langmuir* **2008**, *24*, 3465-3470.

(25) Xiong, B.; Zhou, R.; Hao, J.; Jia, Y.; He, Y.; Yeung, E. S. *Nat. Commun*. **2013**, *4*, 1708.

(26) Park, G.; Lee, C.; Seo, D.; Song, H. *Langmuir* **2012**, *28*, 9003-9009.

(27) Becker, J.; Zins, I.; Jakab, A.; Khalavka, Y.; Schubert, O.; Sönnichsen, C. *Nano Lett.* **2008**, *8*, 1719-1723.

(28) Li, Y.; Li, Z.; Gao, Y.; Gong, A.; Zhang, Y.; Hosmane, N. S.; Shen, Z.; Wu, A. *Nanoscale*, **2014**, *6*, 10631.

(29) Deng, L.; Li, Y.; Yan, X.; Xiao, J.; Ma, C.; Zheng, J.; Liu, S.; Yang, R. *Anal. Chem.* **2015**, *87*, 2452-2458.

(30) Lugg, N. R.; Kothleitner, G.; Shibata, N.; Ikuhara Y. *Ultramicroscopy* **2015**, *151*, 150-159.

(31) Fan, A.; Ling, Y.; Lau, C.; Lu, J. Talanta 2010, 82, 687-692.

(32) Mercury Update: Impact of Fish Advisories. EPA Fact Sheet EPA-823-F-01-011; EPA, Office of Water: Washington, DC, 2001.

(33) Miao, X.; Zou, S.; Zhang, H.; Ling, L. *Sens. Actuators B* **2014**, *191*, 396-400.

(34) Xiang, Y.; Tong, A.; Lu, Y. *J. Am. Chem. Soc.* **2009**, *131*, 15352-15357.

(35) Yildirim, N.; Long, F.; Gao, C.; He, M.; Shi, H.; Gu, Z. A. *Environ. Sci. Technol.* **2012**, 46, 3288-3294.

For TOC